Romanian Reports in Physics, Vol. 62, No. 4, P. 801–810, 2010

BIOPHYSICS

MULTISCALE ANALYSIS OF THE HUMAN BRAIN CORTEX

RADU MUTIHAC

Department of Electricity and Biophysics, University of Bucharest, Romania
E-mail: mutihac@gmail.com

(Received August 29, 2009)

Abstract. The fractal or scale invariant properties demonstrated by neuroimaging data render wavelets appropriate to perform multiresolution analysis according to scale and to optimally process signals that contain various discontinuities and transients by adapting to local or nonstationary features in data within decomposition scales. Processing of functional brain imaging data in the wavelet domain was carried out by means of symmetric biorthogonal functions. Wavelet-based analysis provide natural bases for decorrelation scaling, scale-invariant, and fractal processes in time, space, or both, which are typically encountered in imaging neuroscience.

Key words: fractals, wavelets, multiscale analysis, brain cortex.

1. INTRODUCTION

In data analysis, a frequent task is to find an adequate reduced representation of a multivariate data set for discovery, analysis, and recognition of patterns. Transform domain is a versatile approach widely used in this respect. Major benefits of data processing in an appropriate transform domain are increased mathematical tractability and higher signal-to-noise ratio.

Analysis of functional magnetic resonance imaging (fMRI) data, the most complex biomedical time series, is a noninvasive method that allows to localize and study the dynamic brain processes in intact living brains. Functional brain analysis methods, which reveal statistical regularities in data associated with brain function, can be loosely dichotomized in: (*i*) confirmatory (hypothesis-driven model-based) analysis (CDA) and (*ii*) exploratory (data-driven model-free) analysis (EDA) [1]. In statistical inference, the expected changes in brain activity are specified as regressors within a multiple linear regression framework and the estimated regression coefficients are tested against a null hypothesis. The voxelwise test statistic form summary maps that are representations of the spatial distribution of functional activity induced by some external stimuli [2]. Contrarily, exploratory analysis [3] makes no reference to prior knowledge of data structure and provides models whose characteristics are solely enforced by the statistical properties of data [4].

Multiresolution analysis (MRA) falls somewhat in between since the key features of signals are identified and analyzed with resolutions matched to their scales and subsequently assessed for statistical significance. Wavelets analyze data according to scale, optimally detecting transient events and adapting to local or nonstationary features in data within decomposition scales. Among the wavelet transforms (WT), the continuous wavelet transform (CWT) is commonly applied in physics, whereas the discrete wavelet transform (DWT) is more common in numerical analysis, signal and image processing. The DWT is also applied to statistical analysis of fMRI time series, data resampling by wave-strapping, linear model estimation, and methods for multiple hypothesis testing in the wavelet domain.

Brain function depends on adaptive self-organizing large-scale neural assemblies, which entails some statistical self-similarity of the human cerebral cortex, a property commonly referred to as *fractal*.

2. WAVELETS

2.1. WAVELETS AND SCALING FUNCTIONS

Both for practical and theoretical reasons, wavelets are chosen as *continuously differentiable functions* $f(x)$, $x \in \mathbb{R}$ with *compact support* from a subspace of the space $L_1(\mathbb{R}) \cap L_2(\mathbb{R})$, which is the space of measurable functions that are absolutely and square integrable (e.g., finite energy) in the Lebesgue's sense:

$$\int_{-\infty}^{+\infty} \left| f(x) \right| \mathrm{d}x < +\infty \quad \text{and} \quad \int_{-\infty}^{+\infty} \left| f(x) \right|^2 \mathrm{d}x < +\infty \ . \tag{1}$$

A *Banach* space is a *complete* space endowed with a *norm* of finite or infinite dimension. More generally, one defines the L_p spaces for $1 \leq p \leq +\infty$ (where L stands for Lebesgue) as the set of functions whose L_p-norm:

$$\left\| f \right\|_{L_p} = \left(\int_{-\infty}^{+\infty} \left| f(x) \right|^p \mathrm{d}x \right)^{1/p} . \tag{2}$$

Wavelet analysis adopts two continuously-defined functions:

1. The *scaling function* (or *father function*) $\phi(x)$, which is the solution of a *two-scale* equation:

$$\phi(x) = \sqrt{2} \sum_{k \in \mathbb{Z}} h(k) \phi(2x - k) , \tag{3}$$

where the sequence $\{h(k)\}_{k \in \mathbb{Z}}$ is the *refinement* filter.

2. Its associated *wavelet function* $\psi(x)$ (*prototype* or *mother wavelet* function):

$$\psi(x) = \sqrt{2}\sum_{k\in\mathbb{Z}} g(k)\phi(2x-k) \tag{4}$$

where $\{g(k)\}_{k\in\mathbb{Z}}$ is a suitable weighting sequence.

As such, the conditions of *zero mean* and *square norm one*, respectively, can be easily set:

$$\int_{-\infty}^{+\infty} \psi(x)\mathrm{d}x = 0 \quad \text{and} \quad \int_{-\infty}^{+\infty} |\psi(x)|^2 \mathrm{d}x = 1 . \tag{5}$$

2.2. WAVELET BASIS FUNCTIONS

Wavelet construction starts from $\psi(x)$, which generates the basis by *dilation* (index *j*) and *translation* (index *k*) in time, $\psi(ax-b)$. For the discrete wavelets, the parameter of translation $b = k$ and dilation $a = 2^j$, where $j,k \in \mathbb{Z}$. Dilation allows hierarchical representation of a data set. Temporal analysis is performed with a contracted, high-frequency version of the prototype wavelet, while frequency analysis is performed with a dilated, low-frequency version of the same wavelet:

$$\psi_{j,k} = 2^{-j/2}\psi\left(x/2^{-j} - k\right). \tag{6}$$

The collection of shifted and scaled wavelet functions forms a *wavelet basis*. Any continuous function (e.g., signal or image) is uniquely projected onto the wavelet basis functions and expressed as a linear combination of the basis functions. The set of coefficients which weight the wavelet basis functions in such representation is referred to as the *wavelet transform* of the given function. A repeating pattern in the wavelet coefficients plot is characteristic of a signal that looks similar on many scales. Complex data can be inspected by dilation, which performs “zoom-in” on details. Reversely, details can be suppressed by stretching, which behaves like “zoom-out”; therefore, wavelets are appropriate candidates for data smoothing.

Orthogonal wavelet basis functions can be found by appropriate choice of the sequences $\{h(k)\}_{k\in\mathbb{Z}}$ and $\{g(k)\}_{k\in\mathbb{Z}}$ or, equivalently, setting appropriate functions, ϕ and ψ, such that $\{\psi_{j,k}\}_{j,k\in\mathbb{Z}}$ form an orthonormal basis of $\mathrm{L}_2(\mathbb{R})$:

$$\langle \tilde{\psi}_{j,k}, \psi_{i,k} \rangle = \delta_{j-1} \cdot \delta_{k-l}, \quad i,j,k,l \in \mathbb{Z}, \tag{7}$$

where $\{\tilde{\psi}_{j,k}\}_{j,k\in\mathbb{Z}}$ are the biorthogonal basis functions of $\{\psi_{j,k}\}_{j,k\in\mathbb{Z}}$. Hence, any function $f(x)\in L_2(\mathbb{R})$ can be uniquely represented by the expansion:

$$f(x)=\sum_{j\in\mathbb{Z}}\sum_{k\in\mathbb{Z}}d_j(k)\psi_{j,k}(x)+\sum_{j\in\mathbb{Z}}\sum_{k\in\mathbb{Z}}a_j(k)\phi_{j,k}(x) \tag{8}$$

where the *detail* coefficients, $\{d_j(k)\}_{j,k\in\mathbb{Z}}$, and the *approximation* coefficients, $\{a_j(k)\}_{j,k\in\mathbb{Z}}$, due to orthogonality, are obtained by forming the inner products of the function $f(x)\in L_2(\mathbb{R})$ with the corresponding basis functions:

$$d_j(k)=\langle f,\psi_{j,k}\rangle L_2 \quad \text{and} \quad a_j(k)=\langle f,\phi_{j,k}\rangle L_2, \quad j,k\in\mathbb{Z}. \tag{9}$$

Practically, the decomposition of any function $f(x)\in L_2(\mathbb{R})$ is carried out on a finite number of scales only, say *J*, resulting in:

$$f(x)=\sum_{j\in\mathbb{Z}}^{J}\sum_{k\in\mathbb{Z}}d_j(k)\psi_{j,k}(x)+\sum_{k\in\mathbb{Z}}c_j(k)\phi_{j,k}(x). \tag{10}$$

The wavelet coefficients are efficiently calculated using Mallat's algorithm [5], which is based on a hierarchical application of filterbank decomposition.

Wavelet families and functions provide a rich space in which to search for a wavelet that optimally represents any function of interest. However, desirable properties such as orthogonality, compactness of support, rapid decay, and smoothness impose a variety of restrictions. Wavelets effectively represent functions which have similar characteristics to the wavelet basis functions. Biorthogonal families of wavelets exhibit the property of *linear phase*, which makes them attractive for signal and image reconstruction. Furthermore, by using two distinct wavelets, one for decomposition and the other for reconstruction rather then a single one, extra properties are revealed [6].

3. FRACTALS

In nature, several complex patterns such as coastlines, clouds, plants, or snow flakes, display some similar characteristics. To measure such complex shapes, Mandelbrot introduced the concept of *fractal* back in 1975. Fractals [7] define a class of objects with the characteristic property of self-similarity (or self-affinity), meaning that the statistics describing the structure in time or space of a fractal process remain the same as the process is measured over a range of different scales (or *scale invariant*). More general, a stochastic process $X(t)$, $t > 0$, is called *self-similar* with exponent $H > 0$ of self-similarity if for all $c > 0$, the processes $X(ct)$, $t \geq 0$ and $c^H X(t)$,

$t \geq 0$, have the same finite-dimensional distributions (i.e., scaling of time is equivalent to an appropriate scaling of space). *Fractal dimension* (FD) refers to any of the dimensions used to characterize fractals like capacity dimension, correlation dimension, information dimension, Hausdorff dimension (larger than topological dimension), Lyapunov dimension, Minkowski-Bouligand dimension, and more. Simplistically, FD is the exponent D in $n(\epsilon) = \epsilon^D$, where $n(\epsilon)$ is the minimum number of *open sets* of diameter ϵ needed to cover the set. In this context, fractals are complex, patterned, statistically self-similar or self-affine, scaling or scale-invariant structures with non-integer dimensions and irregularities difficult to be represented by classical (Euclidian) geometry, generated by simple iterative rules widespread in both real and artificial systems.

Fractals are used especially in computer modeling of irregular patterns and structures in natural (environmental) scenes. Spatial frequencies disclose the spatial complexity of natural images following a $1/f$ power spectrum, where higher spatial complexity is increasingly restricted to smaller portions of the scene. However, computer-generated images with $1/f$ power spectra are not necessarily perceived as beautiful.

Wavelet methods are particularly adequate in brain imaging data analysis due to broadly fractal properties exhibited by the brain in space and time. A wavelet *basis* displays fractal properties (Fig. 1) and, therefore, it may naturally play the role of basis in fractal-like data processing. Hence wavelets may be more than just another basis for analysis of functional neuroimaging data [8].

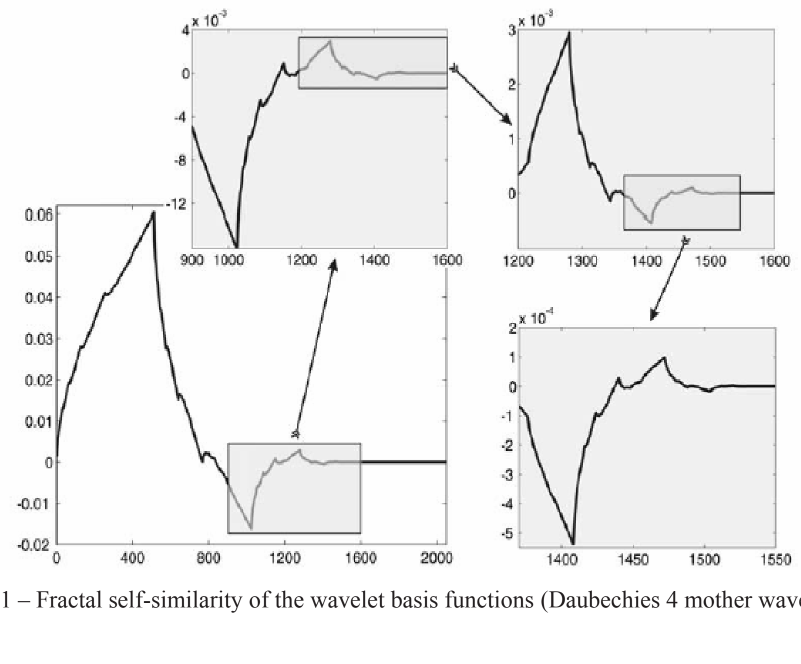

Fig. 1 – Fractal self-similarity of the wavelet basis functions (Daubechies 4 mother wavelet).

4. FRACTAL WAVELET ANALYSIS OF THE BRAIN

4.1. WAVELET-BASED IMAGE ANALYSIS

The WT of an image produces a *multiresolution* representation where each wavelet coefficient contains information on the image at a certain scale in a certain position. In image analysis (like noise reduction, spatial normalization, contrast enhancement, image compression, ...), preprocessing can be carried out by making the operations frequency dependent (i.e., split signal/image into frequency subbands and apply different operations on each subband).

Wavelet methods approach the analysis of statistical fields similarly to images by estimating the signal at any resolution among the random fluctuations. The variance is computed more straightforward for statistical maps than for images because: (*i*) statistical maps are images with noise variance equal to unity; (*ii*) pure noise images (residual images) can be obtained by subtracting from the original scans the effects estimated through statistical analysis. Then the noise power of the field can be computed by Fourier techniques [9]. Variances of wavelet levels are computed by the product of the power function of the field with the power function of the wavelet filters [10]. Therefore, statistical maps are transformed using the DWT, the resulting coefficients are thresholded, and the denoised statistical maps are back-projected by the inverse DTW [11].

Scale-varying wavelet-based methods for hypothesis testing of brain activation maps circumvent the need to specify a priori the size of signals expected and, therefore, the optimal choice of the smoothing kernel required by Gaussian filtering. The high frequency information contained in data is preserved in the wavelet subbands, contrarily to Gaussian filtering in statistical parametric mapping (SPM) based on the general linear model (GLM) [2].

4.2. RESULTS AND DISCUSSION

The temporal autocorrelation function is often transformed into the spectral domain, where the power-law decay for the correlations as a function of time translates into a power-law decay of the spectrum $S(f)$ as a function of frequency and led to terming it $1/f$-like noise. The MR spectrum at low frequency [12] follows the $1/f$ dependence over at least 2 octaves (here from 10 Hz to 40 Hz) with a roll-off rate of about 12 dB/octave (Fig. 2).

The human brain spontaneously generates neural oscillations with a large variability in frequency, amplitude, duration, and recurrence. Nevertheless, the long-term spatiotemporal structure of the complex patterns of the ongoing neural activity is less known, specifically, whether fluctuations in brain activity reflect a memory of the dynamics of the system in the range of a few seconds. It was found that the amplitude fluctuations of low frequency oscillations are correlated and obey $1/f$ power-law scaling behavior referred to as *long memory* effect. The large variability, the long-range correlations, and the power-law scaling behavior of spontaneous oscillations were consistently and unifying explained within the theory of self-organized *criticality*, which provides a general mechanism for the emergence of correlations and complex dynamics in stochastic multiunit systems [13].

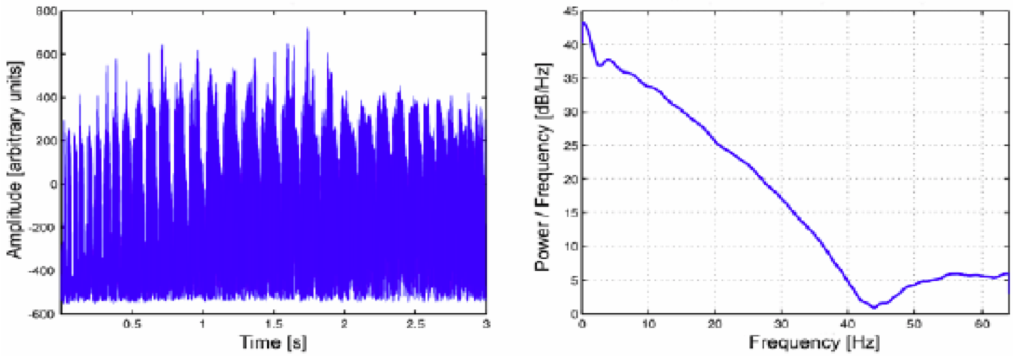

Fig. 2 – Typical fMRI time series (left) and the corresponding MR spectrum at low frequency (right).

Apart from neural population activity, the $1/f$ noise is virtually omnipresent in human beings, such as in heart beat rhythms and statistics of DNA sequences. For very low signal intensities, noise deviation from Gaussianity was evaluated based on the non-parametric Kolmogorov-Smirnoff test as statistically significant in very large images only [14].

In the case of multilevel FWT of *2D* images, the biorthogonal scaling function and its corresponding wavelet function are showed (Fig. 3). These wavelets are also employed to run *2D* three-level WT of an axial MR brain slice (Fig. 4). Further on, the first three approximation levels are presented in sequence (Fig. 5) to facilitate visual inspection.

When the characteristics of a fractal evolve with time and become local, the signal is called a *multifractal*. Brain function depends on adaptive selforganization of large-scale frequency-specific brain functional neural clusters. Human brain functional networks demonstrate a fractal small-world architecture that supports critical dynamics and task-related spatial reconfiguration while preserving global topological parameters [15]. Therefore, wavelets are a particularly suitable tool for practical analysis and generation. Multifractal features of the human brain cortex are revealed by wavelet-based statistical analysis of the fMRI time series acquired in a simple visual task [16].

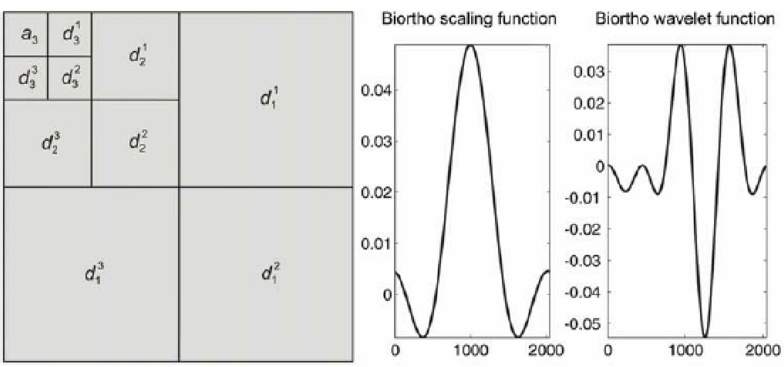

Fig. 3 – Approximation and detailed wavelet coefficients in a level-three *2D* wavelet transform (left); *1D* biorthogonal scaling and wavelet functions, respectively (right).

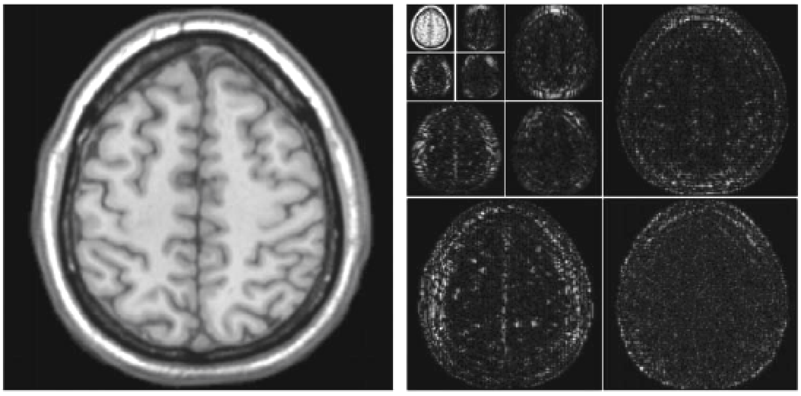

Fig. 4 – An approximation image of a typical MR axial slice at a resolution level L is represented by 2^L pixels in each direction. The *detail* images at particular levels of approximation L are produced by *horizontal*, *vertical*, and *diagonal* differences between successive levels. The set of coefficients produced by the WT consists of the lowest course level image and the higher level detail images.

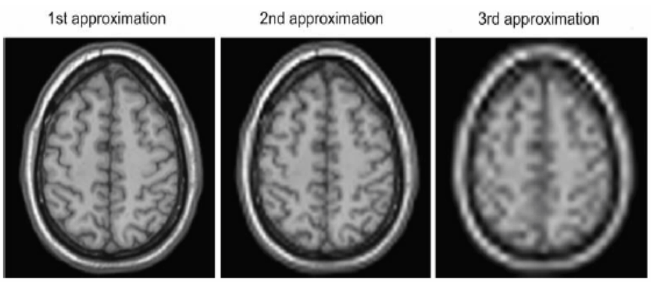

Fig. 5 – Approximation (course) images of a typical MR axial slice at successive resolution levels: 1st approximation $L = 7$ (left); 2nd approximation $L = 6$ (mid); and 3rd approximation $L = 5$ (right). The original image is $2^8 \times 2^8$ pixels and corresponds to resolution $L = 8$. All images are rescaled to the same size for visual convenience.

The preliminary findings so far pointed out that the methods producing smooth images introduce more false positives [14]. Simple nonlinear wavelet methods outperform the traditional linear methods such as Fourier series or kernel-based procedures. The less smoothing wavelet-based methods, though generating more false negatives, produce a smaller total number of errors than Gaussian filtering in the spatial domain. Due to the smoothness of the wavelet representation, the estimated statistical parameter maps reveal more compact regions of activation than their counterparts obtained by statistic testing in spatial domain (Fig. 6).

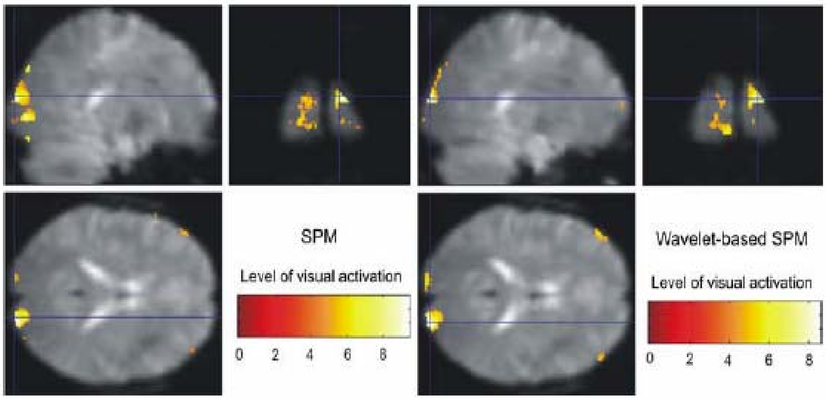

Fig. 6 – Orthogonal view of brain activation parametric maps generated by minimally preprocessed raw fMRI data (left) and wavelet-based statistical analysis (right). In both cases, the multiple hypothesis testing was controlled by false detection rate (FDR) thresholding at statistical significance $q = 0.05$.

5. CONCLUSION

Virtually for all wavelet-based analysis methods, the output SNR is a linear function of the input SNR, that is, the wavelet methods, contrarily to Gaussian smoothing, improve the SNR of the input images that already have a decent SNR. It comes out that the wavelet analysis performs similarly to Gaussian smoothing for low SNR, and better than Gaussian spatial filtering for higher SNR. The high frequency information contained in data is preserved in the wavelet subbands, contrarily to Gaussian filtering in SPM.

Wavelet-based analysis largely matches the fractal properties exhibited by the brain in space and time. It is optimal in terms of detecting transient events in fMRI time series and adapts well to local or nonstationary features in data within the scales of decomposition. The benefits are: (*i*) multiresolution decomposition suitable for scale-invariant processes analysis; (*ii*) optimal decorrelation and Karhunen-Loève expansions for long-memory $1/f$-like processes, which is the case in fMRI; and (*iii*) good estimators for the noise process parameters. Wavelets are mathematically attractive because of *compact support* and their stability with respect to *continuous differentiation* and *integration*. As such, fractal wavelet-based methods are likely to provide an overall richer characterization of distributed brain activation.

Acknowledgements. The author is grateful to Dr. Dimitri Van De Ville, Biomedical Imaging Group, Ecole Polytechnique Fédérale de Lausanne, Switzerland, for clearing up subtleties of the WSPM software, and Dr. John Ashburner, Wellcome Trust Centre for Neuroimaging, University College London, UK for commenting the latest updates in the SPM software package for the analysis of brain imaging data sequences.

REFERENCES

1. L. Mutihac and R. Mutihac, *Mining in chemometrics*, Analitica Chimica Acta, **612,** 1–18 (2008).
2. K.J. Friston, A.P. Holmes, K.J. Worsley, J.-B. Poline, C.D. Frith, and R.S.J. Frackowiak, *Statistical parametric maps in functional imaging*: *A general linear approach*, Hum. Brain. Map., **2**, 189–210 (1995).
3. R. Mutihac and R.C. Mutihac, *A comparative study of independent component analysis algorithms for electroencephalography*, Romanian Reports in Physics, **59**, *3,* 827-853 (2007).
4. R. Mutihac, *Exploratory analysis of auditory modulation in functional magnetic resonance imaging – A case study*, Romanian Reports in Physics, **58**, *4*, 455-480 (2006).
5. S.G. Mallat, *A theory for multi-resolution signal decomposition: The wavelet decomposition*. IEEE Trans. Patter. Anal. Mach. Intell., **11,** 674-693 (1989).
6. D. Van De Ville, T. Blu, and M. Unser, *Surfing the brain: An overview of wavelet-based techniques for fMRI data analysis,* IEEE Engineering in Medicine and Biology Magazine, **25,** *2,* 65–78 (2006).
7. B.B. Mandelbrot, *Les Objets Fractals: Forme, Hasard et Dimension*, Flammarion, Paris, 1975.
8. E. Bullmore, J. Fadili, V. Maxim, L. Sendur, B. Whitcher, J. Suckling, M. Brammer, and M. Breakspear, *Wavelets and functional magnetic resonance imaging of the human brain*, Neuroimage, **23,** S234-S249 (2004).
9. K.J. Worsley, S. Marrett, P. Neelin, A.C. Evans, *Searching scale space for activation in PET images,* Human Brain Map., **4**, 74-90 (1996).
10. F.E. Turkheimer, J.A.D Aston, V.J. Cunningham, *On the logic of hypothesis testing in functional imaging*, European Journal of Nuclear Medicine, **31,** *5,* 725–732 (2004).
11. U.E. Ruttimann, M. Unser, R. Rawlings, D. Rio, N. Ramsey, V. Mattay, D. Hommer, J. Frank, and D. Weinberger, *Statistical analysis of fMRI data in the wavelet domain*. IEEE Trans. Med. Imaging, **17,** *2,* 142–154 (1998).
12. R. Mutihac*, Wavelet-based statistical analysis versus SPM of Brain Imaging Data*. IC-MED, **2**, *3,* 225–236 (2008).
13. K.L. Hansen, V.V. Nikouline, J.M. Palva, and R.J. Ilmoniemi, *Long-range temporal correlations and scaling behavior in human brain oscillations*, J. Neurosci., **21,** *4,* 1370–1377 (2001).
14. A.M. Wink and J.B.T.M. Roerdink, Denoising functional MR images: A comparison of wavelet denoising and Gaussian smoothing. *IEEE Trans. Med. Imaging*, **23,** *3,* 374–387 (2004).
15. D.S. Bassett, A.M.-Lindenberg, S. Achard, T. Duke, and E. Bullmore, *Adaptive reconfiguration of fractal small-world human brain functional networks*, Biological Sciences/Neuroscience, **103**, *51,* 19518–19523 (2006).
16. R. Mutihac, *Exploratory analysis of fMRI data*, *ICTP,* **69**, 1–27 (2004).